Genetic Dissection of Quantitative Trait Loci for Hemostasis and Thrombosis on Mouse Chromosomes 11 and 5 Using Congenic and Subcongenic Strains

Jane Hoover-Plow[*], **Qila Sa**[¤], **Menggui Huang, Jessica Grondolsky**

Department of Cardiovascular Medicine and Department of Molecular Cardiology, Joseph J. Jacobs Center for Thrombosis and Vascular Biology, Clinic, Lerner Research Institute, Cleveland, Ohio, United States of America

Abstract

Susceptibility to thrombosis varies in human populations as well as many inbred mouse strains. Only a small portion of this variation has been identified, suggesting that there are unknown modifier genes. The objective of this study was to narrow the quantitative trait locus (QTL) intervals previously identified for hemostasis and thrombosis on mouse distal chromosome 11 (*Hmtb6*) and on chromosome 5 (*Hmtb4* and *Hmtb5*). In a tail bleeding/rebleeding assay, a reporter assay for hemostasis and thrombosis, subcongenic strain (6A-2) had longer clot stability time than did C57BL/6J (B6) mice but a similar time to the B6-Chr11$^{A/J}$ consomic mice, confirming the *Hmtb*6 phenotype. Six congenic and subcongenic strains were constructed for chromosome 5, and the congenic strain, 2A-1, containing the shortest A/J interval (16.6 cM, 26.6 Mbp) in the *Hmtb4* region, had prolonged clot stability time compared to B6 mice. In the 3A-2 and CSS-5 mice bleeding time was shorter than for B6, mice confirming the *Hmtb5* QTL. An increase in bleeding time was identified in another congenic strain (3A-1) with A/J interval (24.8 cM, 32.9 Mbp) in the proximal region of chromosome 5, confirming a QTL for bleeding previously mapped to that region and designated as *Hmtb10*. The subcongenic strain 4A-2 with the A/J fragment in the proximal region had a long occlusion time of the carotid artery after ferric chloride injury and reduced dilation after injury to the abdominal aorta compared to B6 mice, suggesting an additional locus in the proximal region, which was designated *Hmtb11* (5 cM, 21.4 Mbp). CSS-17 mice crossed with congenic strains, 3A-1 and 3A-2, modified tail bleeding. Using congenic and subcongenic analysis, candidate genes previously identified and novel genes were identified as modifiers of hemostasis and thrombosis in each of the loci *Hmtb*6, *Hmtb*4, *Hmtb*10, and *Hmtb*11.

Introduction

Cardiac and peripheral vascular diseases are the leading cause of death, with thrombosis as the precipitating event. Numerous studies [1-6] show that inherited risk factors contribute significantly to the development of acute myocardial infarction, ischemic stroke, atherosclerosis, thromboembolism and peripheral arterial occlusion. Progress has been made in diagnosis and treating these diseases, but only few of the genetic factors has been identified that explain thrombosis variation.

Approaches to identify genetic determinants of phenotypic traits have advanced rapidly in the last 15 years. Previously, identification relied on single gene spontaneous mutations that

caused an overt phenotype [7-9]. The development of strategies to delete or insert human genes into mice led to the association of specific gene products with specific phenotypes [10-12]. Results of some of these deletions or insertions were surprising; in some cases, there was no obvious phenotype where one was anticipated, and in others, unanticipated phenotypes arose. In addition, murine strain backgrounds were shown to modify the phenotypes of expressed genes [13,14]. With the realization that most common chronic diseases in humans, such as atherosclerosis, obesity or diabetes, are multigenic with more than one gene and even unanticipated gene interactions contributing to disease, new approaches for gene identification and characterization were needed. The development of statistical analyses packages to map complex

traits in mice has provided an approach to such complex diseases [15]. These approaches allow for the mapping of loci of genes that contribute quantitatively to a particular phenotype or pathology, a quantitative trait locus (QTL) [16]. The loci of a number of genes for obesity [17-21] and atherosclerosis [22-28] have been successfully mapped by such QTL analyses. The first step in QTL analysis is the identification of two phenotypically disparate strains, performing the strain intercross, and phenotyping and genotyping F2 progeny. Both inbred strains and recombinant congenic strains (strains with essentially the same background except for selective differential chromosomal segments) [29], have been used in such QTL mapping. Only a few studies [14,30] have investigated risk factors for thrombotic disease using mouse genetic approaches.

An approach that we have utilized is to analyze QTL with the chromosome substitution strains (CSS) [31]. In consomic strains the differential variation is a whole chromosome rather than just a chromosomal segment. This approach has been applied to the B6 and A/J mice, which have been characterized to have differences in many traits [32,33]. A panel of 21 CSS was constructed by a "marker-assisted" breeding program. Each of the 21 chromosomes were substituted individually with an A/J chromosome [34] into the B6 background. Often many more QTL are identified with the CSS than with genome-wide scans. In a previous study [35], we found that the two inbred strains, C57BL/6J (B6) and A/J, had marked differences in hemostatic and thrombotic responses. In a tail bleeding/ rebleeding assay, rebleeding time (clot stability) was longer in A/J mice compared to B6 mice. In addition, A/J mice had a rapid occlusion time after $FeCl_3$ injury of the carotid and reduced patency. The tail bleeding/rebleeding assay, a reporter of hemostasis and thrombosis, was used as screening assay for a panel of consomic strains (B6-Chr1-19, X, Y$^{A/J}$), which had one chromosome from A/J mice in a B6 background [35]. The B6-Chr11$^{A/J}$ (CSS-11) and B6-Chr5$^{A/J}$ (CSS-5) had a phenotype similar to A/J mice, long clot stability. We identified the QTLs, *Hmtb6*, *Hmtb4*, and *Hmtb5*, for hemostasis and thrombosis on mouse chromosomes 11 and 5 in an F$_2$ intercross from CSS-11 X B6 and CSS-5 X B6 [36]. The goal of this study was to fine map the QTLs, *Hmtb6*, *Hmtb4*, and *Hmtb5*, using congenic and subcongenic mouse strains. Here we report confirmation of the QTLs for clot stability in *Hmtb6* and *Hmtb4* and the QTL for bleeding in *Hmtb5*. In addition, another QTL for bleeding, *Hmtb10*, and a QTL for carotid occlusion time after injury, *Hmtb11*, were identified in the proximal region.

Materials and Methods

Mice

The parental inbred mouse strains C57BL/6J (B6, 000664) and A/J (000646), and the C57BL/6J-Chr 5A/J/NaJ (CSS-5, 004383) and C57BL/6J-Chr 11A/J/NaJ (CSS-11, 004389) mouse strains were purchased from the Jackson Laboratory (Bar Harbor, ME) and maintained in the Biological Resources Unit facility at the Cleveland Clinic. Congenic and subcongenic strains were generated from CSS-5 and CSS-11 consomic mice using marker-assisted backcrossing [31]. Mice were

housed in sterilized isolator cages with a 14hr/10hr light/dark cycle and ad libitum access to water and food. The bleeding/ rebleeding assay was performed on both male and female mice at 6-9 wk. of age. The Cleveland Clinic Institutional Animal Care and Use Committee approved this study and procedures were followed in accordance with institutional guidelines.

Genotyping

Genomic DNA was prepared from ear punches of the mice and genotyping performed using polymerase chain reaction (PCR) for microsatellite markers (Mouse Mappairs, Invitrogen, Carlsbad, CA). PCR was performed using HotstarTaq Master Mix Kit (QIAGEN, Valencia, CA). The PCR products were detected by electrophoresis on 10% polyacrylamide gels (National Diagnostics, Atlanta, GA) and visualized by ethidium bromide staining. Microsatellite markers and primers for the RLF markers were used to identify mice by marker assisted selection [31,34] (Tables S1 and S2). Marker and genomic coordinates of genes were determined from the Mouse Genome Database (MGD), 2012 [37]. The following terms were used for the annotated analysis: hemostasis, thrombosis, clotting, platelets, fibrinolysis, bleeding, blood and coagulations. Genes were subjected to functional annotation programs, David Bioinformatics Resources 6.7 (http:// david.abcc.ncifcrf.gov/home.jsp) [38] and the MGD, 2012 [37].

Tail Bleeding/Clot Stability Assay

Phenotyping was performed using the bleeding/rebleeding assay as previously described [35]. The mice were anesthetized with ketamine/xylazine (90 mg/kg, 10 mg/kg), the tail prewarmed for 5 minutes in 10 mL of saline at 37°C in a water bath. The tail was lifted from the saline and a 5 mm tail segment amputated and immediately returned to the saline. Bleeding time was measured as the time between the start of the bleeding and cessation of the bleeding. Clot stability time was measured as the time between the cessation of the bleeding and the start of the second bleeding.

FeCl$_3$-induced Carotid Injury model

To induce thrombus formation in the carotid artery, a ferric chloride ($FeCl_3$) model of vessel injury was employed as previously described [35]. Mice were anesthetized with ketamine/xylazine (90 mg/kg, 5 mg/kg), a midline cervical incision was made and the left common carotid artery isolated by blunt dissection. The flow probe (Transonic Systems, model 0.5PSB) was placed under the artery and when a stable baseline was reached, a 0.5 × 2 mm strip of filter paper saturated with 10% $FeCl_3$ solution was applied to the surface of the carotid artery for 3 minutes. Occlusion time was determined from the addition of the $FeCl_3$ solution to the occlusion of the artery (minimum blood flow). There was no difference in baseline blood flow data in carotid arteries among the mouse strains. The flow probe (Model 0.5PSB,Transonic Systems, Ithaca, NY) was in place from baseline measurements to several minutes after the stable occlusion had been reached, or stopped at 30 min if it had not occluded. Blood flow was recorded every 10 sec (Model TS420, Transonic Systems).
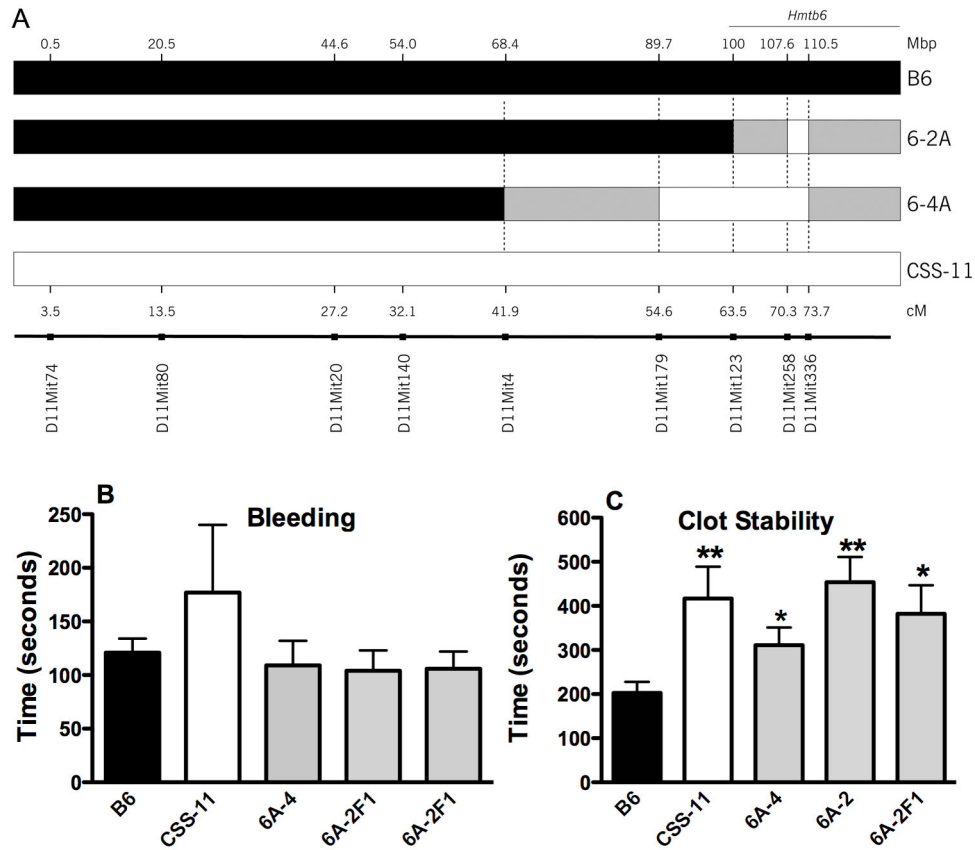
Figure 1. Genotype of Chromosome 11 Congenic and Subcongenic Mice. A. Marker positions. White bars-A/J, grey-uncertain, black-B6. B. First bleeding. C. Time between first and second bleeding. Values are the mean ± SEM, n=10-28, one-way ANOVA, * P< 0.05, **P<0.01.

doi: 10.1371/journal.pone.0077539.g001

CaCl$_2$ Abdominal Aorta Induced Aneurysm (AAA) Formation

AAA was induced by periaortic application of CaCl$_2$ [39]. Mice at age 6~8 weeks were anesthetized (90mg /kg ketamine/ 5mg/kg xylazine) and the abdominal aorta between the renal arteries and bifurcation of the iliac arteries was isolated from surrounding tissue. An image of the aorta was acquired by Spot Image 4.0.3 through a cooled CCD camera attached to an Olympus SZ-PT dissection microscope. After image acquisition, cotton gauze (1 x 0.5 cm) that had been soaked in 0.5 M CaCl$_2$ solution was applied to the external surface of the aorta. After 10 minutes the aorta was rinsed with 0.9% sterile saline and the incision was closed. Three weeks later, after the mice were anesthetized and the aorta exposed after dissecting away the surrounding fatty tissue and scarring adhesions, images were collected as above. The aorta diameter was measured from the before and after CaCl$_2$ images by ImagePro software.

Statistics

Data are presented as the mean ± SEM. One-way ANOVA and Newman-Kuels post-test were used to determine statistical differences between groups. A P value of <0.05 was considered significant.

Results

Chromosome 11 Congenic and Subcongenic Strains

Our previous study, using F2 progeny from a cross of CSS-11 and B6, identified a QTL for clot stability time in the bleeding/rebleeding assay on mouse distal chromosome 11 that peaked at the genetic marker *D11Mit336* [36]. To verify this QTL (*Hmtb6*), congenic strains were constructed by crossing the CSS-11 mice and B6 mice to produce the congenic strain 6A-4 and the subcongenic strain 6A-2. The position of the A/J regions is indicated in Figure 1A, and boundary markers are summarized in Table 1. The minimum congenic interval is the interval between markers with A/J genotypes on the B6 background. The maximum interval is the interval between two markers with B6 genotypes just outside the minimum interval. The interval between minimum and maximum intervals are of unknown genotype [29]. The minimum A/J interval for 6A-4 is 20.8 Mbp, and for 6A-2, 2.9 Mbp.

Table 1. Summary of Congenic and Subcongenic Strains.

Strain	Markers	Marker Positions(cM)	Region (cM)	Marker Positions(Mbp)	Region (Mbp)
Minimum					
Chromosome 11					
6A-4	*D11Mit179-D11Mit336*	54.6-73.7	19.1	89.7-110.5	20.8
6A-2	*Dmit258-D11mit336*	70.3-73.7	3.4	107.6-110.5	2.9
Chromosome 5					
6A-1	*rs1680965-D5Mit338*	5-53.2	48.2	21.4-108.6	87.2
4A-2	*rs1680965-D5Mit197*	5-32.9	27.9	21.4-64.6	43.2
3A-1	*rs16809655-D5Mit394*	5-29.8	24.8	21.4-54.3	32.9
4A-1	*D5Mit394-D5Mit338*	29.8-53.2	23.4	54.3-108.6	54.3
3A-2	*rs6297441-D5Mit320*	48.6-65.2	16.6	100.2-126.8	26.6
2A-1	*D5Mit338-D5Mit320*	53.2-65.2	12	108.6-126.8	18.2
Maximum					
Chromosome 11					
6A-4	*D11Mit4-*	41.9-88	80.1	68.4-122	53.6
6A-2	*D11Mit123-*	63.5-88	58.5	100-122	22
Chromosome 5					
6A-1	*—D5Mit320*	0-65.2	65.2	0-126.8	126.8
4A-2	*—rs6297441*	0-48.6	48.6	0-100.2	100.2
3A-1	*—D5Mit197*	0-32.9	32.9	0-64.6	64.6
4A-1	*D5Mit13-D5Mit320*	20-65.2	45.2	37.4-126.8	89.4
3A-2	*DMit197-rs13478553*	32.9-77	44.1	64.6-138.8	74.2
2A-1	*rs6297441-rs13478553*	48.6-77	28.4	100.2-138.8	38.6

The minimum congenic interval is the interval between markers with A/J genotypes on the B6 background. The maximum interval is the interval between two markers with B6 genotypes just outside the minimum interval. The interval between minimum and maximum intervals are of unknown genotype [29]. Marker and genomic coordinates were determined from the Mouse Genome Database (MGD), 2012 [37].

doi: 10.1371/journal.pone.0077539.t001

Bleeding Time in Chromosome 11 Congenic and Subcongenic Mice

The homozygous congenic and subcongenic mice were phenotyped using the tail bleeding/rebleeding assay as described in the Methods. The higher bleeding time value for CSS-11 mice was not statistically significant (P > 0.05) compared to B6 mice, and the bleeding times in 6A-4 mice and 6A-2 mice were similar to the bleeding time in the B6 mice (Figure 1B).

Clot Stability Time in Chromosome 11 Congenic and Subcongenic Mice

Similar to the CSS-11 parental strain (417±71 sec, n=10), the congenic mice (6A-4) exhibited significantly longer (P<0.05) clot stability times (311±40 sec, n=27) compared to the B6 strain (203±25 sec, n=27) (Figure 1C). The clot stability time was 53% longer in the congenic strain than for B6. To further narrow the QTL interval, a subcongenic strain, 6A-2, was developed (Figure 1A, Table 1). The clot stability time (454 ± 57 sec, n=12) in this subcongenic strain mice was 2.2-fold longer (P=0.01) compared to B6 mice (Figure 1C), and compared to B6 mice, the 2A strain accounts for 100% of the increase in clot stability time for CSS-11, whereas the 4A strain accounts for only 50% of the increase suggesting the trait is isolated to the *D11Mit258* to *D11Mtt336* region. Although the

region from *D11Mit258* and *D11Mit336* was genotyped as A/J, we cannot completely rule out the uncertain regions as harboring the gene(s) responsible for the phenotype of long clot stability. Hmtb6-2A F1, clot stability time (382 ± 65, n=11), was 2-fold longer (P=0.05) than for B6 mice, suggesting dominant inheritance of the QTL. These results demonstrate that this distal region on chromosome 11 contains a genetic factor (or factors) that dominantly controls the clot stability time. This *Hmtb*6 QTL was narrowly mapped to a minimum region of 2.9 Mbp. In this region 107.6-110.5 Mbp region on Chromosome 11 there are 25 protein-coding genes (Table S3, blue area) and when the two adjoining regions of uncertain genotype were included, there are 429 genes (Table S3). Annotation of these genes Identified 14 genes additional genes related to hemostasis, thrombosis, clotting, platelets, coagulation, bleeding, blood, or fibrinolysis (Table 2). The genes in the A/J fragment are *Abca5*, *Apoh*, *Gna13*, and the genes in the regions of uncertain genotype are *Ace*, *Adam11*, *Cntnap1*, *Gjc1*, *Itga2b*, *Itgb3*, *Pecam1*, *Plcd3*, *Cd300lf*, *Hn1*, and *Jmjd6* (Table 2A).

Chromosome 5 Congenic and Subcongenic Strains

Congenic and subcongenic strains were constructed to verify the overlapping QTL on chromosome 5, *Hmtb*4 and *Hmtb*5, for clot stability and bleeding. Congenic strain 3A-2 and

Table 2. Candidate Genes for Thrombosis Modifiers on Chromosome 11 and Chromosome 5.

cM	Genome Coordinates (Mbp)	Symbol, Name
A. Hmtb6, Chromosome 11, 107.6-110.5 Mbp, 70.3-73.7 cM		
68.84	105967945-105989964 (+)	*Ace*, angiotensin I converting enzyme (peptidyl-dipeptidase A) 1
66.48	109362831-109401369 (+)	*Adam11*, a disintegrin and metallopeptidase domain 11
64.33	110269369-110337716 (-)	*Cntnap1*, contactin associated protein-like1
66.48	102799579-101190724 (-)	*Gjc1*, gap junction protein, gamma 1
66.29	102453297-102470122 (-)	*Itga2b*, integrin alpha 2
67.84	104608000-104670476 (+)	*Itgb3*, integrin beta 3
69.92	106654217-106750628 (-)	*Pecam1*, platelet/endothelial cell adhesion molecule 1
66.71	103070304-103101658 (-)	*Plcd3*, phospholipase C, delta 3
73.53	110269369-110337716 (-)	*Abca5*, ATP-binding cassette, sub-family A (ABC1), member 5
71.80	108343354-108414396 (+)	*Apoh*, apolipoprotein H, beta-2-glycoprotein 1
71.88	109362831-109401369 (+)	*Gna13*, guanine nucleotide binding protein, alpha 13
80.59	115116214-115133992 (-)	*Cd300lf*, CD300 antigen like family member F
80.84	115497353-115514387 (-)	*Hn1*, hematological and neurological expressed sequence 1
81.49	116837432-116843449 (-)	*Jmjd6*, jumonji domain containing 6
B. Hmtb5, Chromosome 5, 100.2-108.6 Mbp, 48.6-65.2 cM		
50.45	103692374-103855322 (+)	*Affl*, AF4/FMR2 family, member 1
52.23	107716657-107726036 (-)	*Gfi1*, growth factor independent 1
52.23	107548967-107597888 (-)	*Glmn*, glomulin, FKBP associated protein
48.51	100679484-100719716 (-)	*Hpse*, heparanase
53.13	108461232-108506976 (+)	*Pcgf3*, polycomb group ring finger 3
53.07	108388391-108506976 (+)	*Pde6b*, phosphodiesterase 6B, cGMP, rod receptor, beta polypeptide
50.68	104459450-108432397 (+)	*Pkd2*, polycystic kidney disease 2
48.49	100553725-100572245 (-)	*Plac8*, placenta-specific 8
50.43	103425192-103598359 (+)	*Ptn13*, protein tyrosine phosphatase, non-receptor type 13
50.68	104435118-104441050 (+)	*Spp1*, secreted phosphoprotein 1
51.9	107106570-107289629 (-)	*Tgfbr3*, transforming growth factor, beta receptor III
C. *Hmtb10*, Chromosome 5, 21.4-54.3 Mbp, 5-29.8 cM		
17.9	34573664-34632308 (+)	*Add1*, adducin 1 (alpha)
19.24	36747374-36748679 (-)	*Bloc1s4*, biogenesis of organelles complex-1, subunit 4, cappuccino
17.52	33247724-33275004 (-)	*Ctbp1*, C-terminal binding protein 1
20.4	38319509-38322310 (+)	*Drd5*, dopamine receptor D5
16.9	30913402-30921278 (-)	*EMILIN1*, elastin microfibril interfacer1
23.81	43744616-43821639 (-)	*Fbxl5*, F-box and leucine-rich repeat protein 5
17.27	31253280-31291114 (-)	*Ift172*, intraflagellar transport 172
10.33	23434441-23504235 (+)	*Mll5*, myeloid/lymphoid or mixed-lineage leukemia 5
20.21	37820485-37824583 (-)	*Msx1*, homeobox, msh-like 1
11.32	24364810-24384474 (+)	*Nos3*, nitric oxide synthase 3, endothelial cell
29.37	53590215-53657445 (+)	*Rbpj*, rcombination signal binding protein for immunoglobulin kappa 3 region
11.93	24802823-24842624 (-)	*Rheb*, Ras homolog enriched in brain
14.39	28456815-28467101 (-)	*Shh*, sonic hedgehog
17.06	31116712-31137630 (+)	*Trim54*, tripartite motif-containing 54
20.63	38526813-38561595 (-)	*Wdr1*, WD repeat domain 1
D. *Hmtb4*, Chromosome 5,108.6-126.8 Mbp, 53.2-65.2 cM		
61.84	121950106-121952989 (-)	*Adam1a*, a disintegrin and metallopeptidase domain 1a
61.83	121950107-121953444 (-)	*Adam1b*, a disintegrin and metallopeptidase domain 1b
60.64	120680202-120711927 (-)	*Dtx1*, deltex 1 homolog (Drosophila)
57.92	118064981-118155458 (-)	*Fbxw8*, F-box and WD-40 dommain protien 8
54.69	112343083-112378414 (+)	*Hps4*, Hermansky-Pudlak syndrome 4 homolog (human)
62.63	122870668-123015080 (-)	*Kdm2b*, lysine (K)-specific demethylase 2B
56.09	115429599-115455698 (+)	*Msi1*, musashi RNA-binding protein 1
62.16	122100951-122113472 (+)	*Myl2*, myosin, light polypeptide 2, regulatory, cardiac, slow
54.8	112688876-112896362 (-)	*Myo18b*, myosin XVIIIb
57.29	117781032-117958840 (+)	*Nos1*, nitric oxide synthase 1, neuronal

Table 2 (continued).

cM	Genome Coordinates (Mbp)	Symbol, Name
62.72	123015074-123030450 (+)	*Orai1*, ORAI calcium release-activated calcium modulator 1
53.49	110339812-110343035 (-)	*P2rx2*, purinergic receptor P2X, ligand-gated ion channel, 2
62.53	122707584-122729738 (+)	P2rx4, purinergic receptor P2X, ligand-gated ion channel, 4
61.72	121130533-121191397 (-)	*Ptpn11*, protein tyrosine phosphatase, non-receptor type 11
55.59	113817798-113830501 (-)	*Selplg*, selectin, platelet (p-selectin) ligand
61.99	121815488-121836859 (-)	*Sh2b3*, SH2B adaptor protein 3
60.34	119670862-119684724 (+)	*Tbx3*, T-box 3
63.03	123528764-123573015 (-)	*Vps33a*, vacuolar protein sorting 33A (yeast)
E. Hmtb 11, Chromosome 5, 0-21.4 Mbp.		
3.43	8660077-8748575 (+)	*Abcb1a*, ATP-binding cassette, sub-family B (MDR/TAP), member 1A
3.43	8798147-8866314 (+)	*Abcb1b*, ATP-binding cassette, sub-family B (MDR/TAP), member 1B
3.43	8893721-8959225 (+)	*Abcb4*, ATP-binding cassette, sub-family B (MDR/TAP), member 4
2.26	3928054-4080209 (+)	*Akap9*, A kinase (PRKA) anchor protein (yotiao) 9
8.11	17781690-17888959 (-)	*Cd36*, CD36 antigen
2.04	3344312-3522225 (+)	*Cdk6*, cyclin-dependent kinase 6
2.3	4081145-4104746 (-)	*Cyp51*, cytochrome P450, family 51
3.69	9118801-9161749 (-)	*Dmtf1*, cyclin D binding myb-like transcription factor 1
9.83	21372642-21378374 (+)	*Fgl2*, fibrinogen-like protein 2
2.61	4753873-4758035 (-)	*Fzd1*, frizzled homolog 1 (Drosophila)
7.07	16553550-16619439 (+)	*Hgf*, hepatocyte growth factor
2.26	3803165-3844515 (+)	*Krit1*, KRIT1, ankyrin repeat containing
9.83	20986645-21055911 (-)	*Ptpn12*, protein tyrosine phosphatase, non-receptor type 12
4.31	13396784-13602565 (+)	*Sema3a*, sema domain, immunoglobulin domain (Ig), short basic domain, secreted, (semaphorin) 3A
7.99	17574281-17730268 (+)	*Sema3c*, sema domain, immunoglobulin domain (Ig), short basic domain, secreted, (semaphorin) 3C
5.66	14025276-14256689 (+)	*Sema3e*, sema domain, immunoglobulin domain (Ig), short basic domain, secreted, (semaphorin) 3E
3.37	7960472-7982213 (+)	*Steap4*, STEAP family member 4

Protein coding genes of QTL intervals annotated were subjected to functional annotation programs, David Bioinformatics Resources 6.7 (http://david.abcc.ncifcrf.gov/home.jsp) [38], from the Mouse Genome Database (MGD), 2012 [37]. Annotation search words–hemostasis, thrombosis, clotting, platelets, coagulation, bleeding, blood, fibrinolysis. Shaded areas are genes of uncertain genotype.

doi: 10.1371/journal.pone.0077539.t002

subcongenic strain 2A-1 were constructed for the distal region of chromosome 5 containing the *Hmtb4* and *Hmtb5* QTL peak markers (Table 1, Figure 2). In the QTL analysis there was a suggestive peak for bleeding in the proximal region of chromosome 5, and subcongenic strains 4A-1, 4A-2, and 3A-1 were constructed from the 6A-1 congenic strain for this region of chromosome 5 (Table 1, Figure 2).
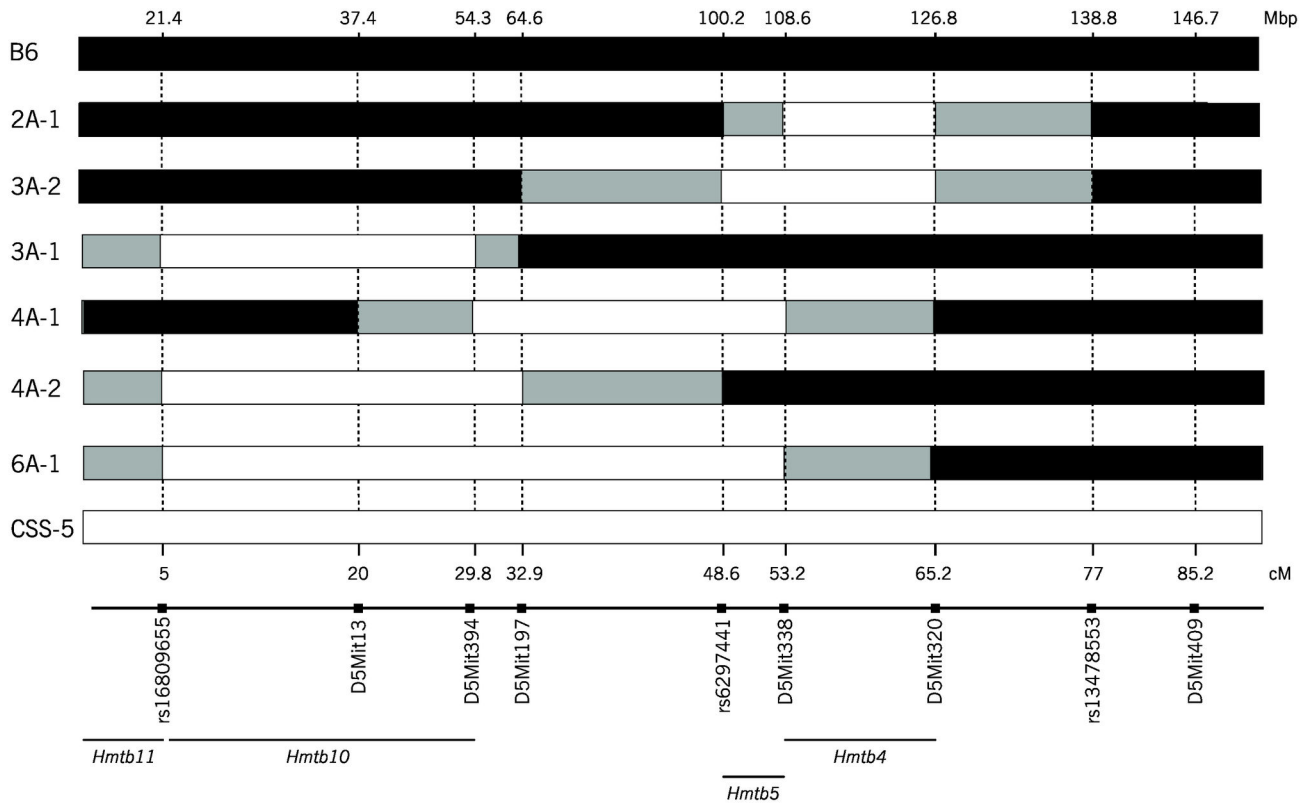
Bleeding Time in Chromosome 5 Congenic and Subcongenic Strains

Bleeding time in the CSS-5 mice (63±7, n=7) was significantly shorter than for B6 mice (121±13, n=28) as previously reported [35] and the congenic strain, 3A-2 (60±9, n=17) also had the same phenotype. The A/J fragment of 3A-2 strain was slightly longer than for the 2A-1 strain with an additional 35.6 Mbp region between *D5Mit197* and rs6297441 (Table 1). The bleeding time of the 2A-1 was the same as the time in B6 mice suggesting the additional region of 3A-2 harbored the short bleeding time. This narrow region of 3A-2

may be the site for the CSS-5 short bleeding time phenotype (Figure 3A), and the *Hmtb5* locus identified in the QTL mapping [36]. Thus, for the *Hmtb5* locus, the minimum A/J interval on 3A-2 strain, 100.2-108.6 Mbp that did not overlap with 2A-1, there are 78 protein-coding genes (Table S4), and functional annotation analysis revealed 11 relevant genes (Table 2).

In the proximal region of chromosome 5, bleeding times for the subcongenic strains 4A-2 and 4A-1 mice were similar to B6 mice (Figure 3A). The 3A-1 mice, carrying the A/J interval from the proximal end to the marker *D5Mit394*, had a longer bleeding time (251±51, n=15, P< 0.01) that was 2-fold longer than A/J or B6 mice (Figure 3A). This suggests an additional locus for bleeding time on chromosome 5 and is consistent with the QTL analysis that identified a suggestive locus at the proximal end of the chromosome. This locus was named *Hmtb10* with the minimum interval of 32.9 Mbp. There are 266 protein-coding genes (Table S5), and the annotation analysis identified 15 genes (Table 2). Thus, there are two loci on chromosome 5 for bleeding, one in the distal region (Hmtb5) and one in the proximal region (*Hmtb10*).

Figure 2. Genotype of Chromosome 5 Congenics and Subcongenic Mice. Marker positions. White bars-A/J, grey-uncertain, black-B6, hatched-heterozygous.
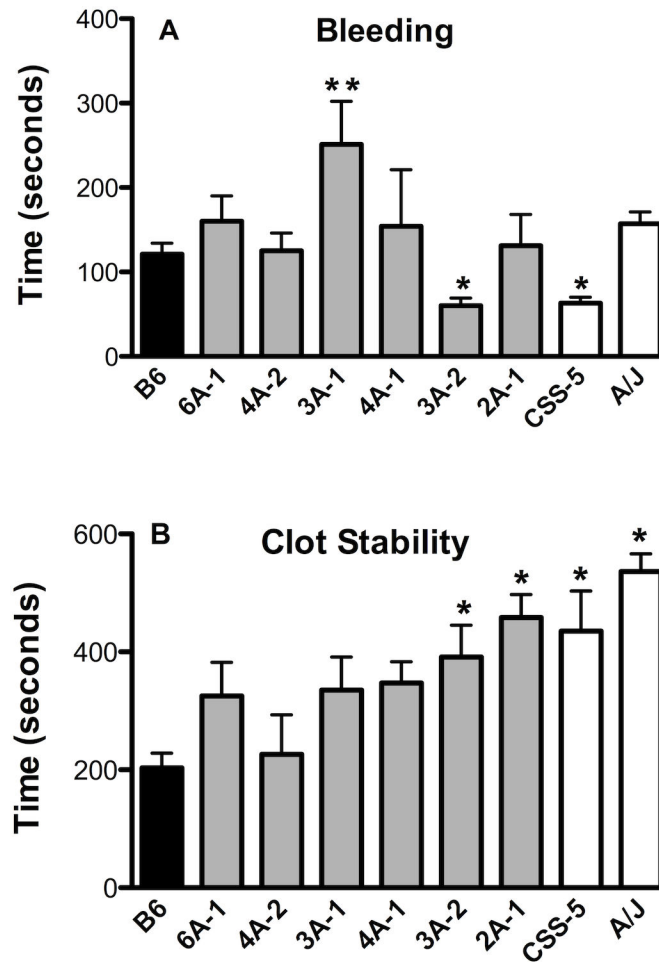
doi: 10.1371/journal.pone.0077539.g002

Clot Stability Time in Chromosome 5 Congenic and Subcongenic Strains

The subcongenic strain with the smallest A/J interval, 2A-1, had significantly prolonged clot stability time (458±39, n=16), comparable to the CSS-5 parental strain (Figure 3B) and confirms the *Hmtb4* locus on chromosome 5 with the minimum interval of 18.2 Mbp (Figure 2, Table 1). Although 6A-1 (325±57, n=11), 4A-1 (347±47, n=7) and 3A-2 (335±58, n=13) mice had long clot stability times, none of the values were significantly different from the B6 mice (Figure 3B). The subcongenic strain 4A-2 had a clot stability time (226±67, n=7) similar to B6 mice. These data suggest that the distal region of chromosome 5 is the site of the clot stability time (*Hmtb4*). In the region of 108.6-126.8 Mbp on chromosome 5, interval of A/J minimum genotype on 3A-2 strain, there are 272 protein-coding genes (Table S6). Functional annotation analysis identified 18 relevant genes (Table 2).

Carotid and Abdominal Aorta Vascular Injury

Hemostasis and thrombosis are complex polygenic processes. While QTL link genomic regions to phenotypic data, multiple traits within the QTL region may be responsible for a particular phenotype [40-42]. To further characterize the phenotype of the *Hmtb4*, *Hmtb5*, and *Hmtb10* loci, carotid occlusion time after $FeCl_3$ injury (Figure 4A) and abdominal aortic aneurysm formation after $CaCl_2$ injury (Figure 4B) were assessed in the congenic strains. In the carotid vascular injury model, a thrombus forms and occludes blood flow. The time required for the occlusion time can detect imbalances in coagulation and platelet functions. The strains 6A-1, 3A-1 and 3A-2, had occlusion times that were not statistically different from B6 or CSS-5 mice (Figure 4A), but the values for 3A-1 and 3A-2 mice were closer to the CSS-5 mice. The 4A-2 strain had a prolonged occlusion time that was 4-fold longer than B6 mice (P < 0.01) and similar to the CSS-5 strain. In addition, the 4A-2 strain had the lowest response to the $CaCl_2$ injury and the increase in diameter of the congenic was similar to the CSS-5 mice. The results of these two models, carotid injury and abdominal aorta injury, revealed that another locus, related to thrombosis modification, occurs within this region on chromosome 5, Hmtb11. Compared to 3A-1 mapped at *rs1680965* and *D5Mit394*, the 4A-2 congenic was genotyped at *rs1680965* and *D5Mit197*, only a difference of 10 Mbp. Within this additional region there were only 10 additional protein coding genes and they did not associate with the annotation criteria (Table S7). One possibility is that the regions from 0-21.4 Mbp (rs1680965) in the two congenic strains, 3A-1and 4A-2, were genetically different. In this region (0-21.4 Mbp) there are 89 protein-coding genes (Table S8). Annotation analysis identified 17 genes in this region (Table 2).

Figure 3. Tail Bleeding/Rebleeding Assay. A. First bleeding time. B. Clot Stability-time between first and second bleeding. Values are the mean ± SEM, n=7-28. One-way ANOVA, *P < 0.05, ** P < 0.01.
doi: 10.1371/journal.pone.0077539.g003

CCS-17 Backcross with Chromosome 5 Congenics

Previously, we reported an interaction of the genes on chromosome 5 and chromosome 17 that modified bleeding and clot stability in the tail bleeding/rebleeding assay [35]. To test if we could determine if this interaction was in the proximal or distal region on chromosome 5, the 3A-1 (proximal) mice and 3A-2 (distal) mice were crossed with CSS-17 mice (Figure 5A). When the 3A-1 mice with the long bleeding times were crossed with CSS-17 mice, the 17 x 3A-1 mice now had short bleeding times (60±9, n=9) suggesting an inhibition by chromosome 17 on the long bleeding times of 3A-1 mice. When the 3A-2 mice with the short bleeding times were crossed with CSS-17 mice, the 17 x 3A-2 mice had longer bleeding times (115±31, n=24) compared to the 3A-2 mice suggesting an interaction of chromosome 17 with this region. Thus, the genes of A/J chromosome 17 interacted with *Hmtb5* and *Hmtb10* of chromosome 5 to modify bleeding time.

For clot stability time (Figure 5B), there was no difference between, the 3A-2 and 17 x 3A-2 or between 3A-1 and 17 x 3A-1. The clot stability time in the F1 progeny of the CSS-5 and CSS-17 mice was similar to the value for B6 mice [35], and in the cross of CSS-17 and CSS-5 (17 x 5) the long clot stability time was recovered. Taken together this suggests that long clot stability time requires two alleles for expression, two in the CSS-5 or two from CCS-17 or one allele from each. The one allele from chromosome 17 and either the locus *Hmtb5* (3A-2) or *Hmtb10* (3A-1) in the cross were sufficient for the expression of the phenotype.

Discussion

In this study, we confirmed the previously identified QTL, *Hmtb6*, *Hmtb4*, and *Hmtb5* for hemostasis and thrombosis on mouse chromosomes 11 and 5 in congenic and subcongenic strains. Two additional QTL have also been identified, *Hmtb*10 and *Hmtb*11. To our knowledge, this is the first study to confirm QTLs associated with hemostasis and thrombosis using congenic and subcongenic mouse strains. Figure 6 summarizes the QTL and potential candidate genes.
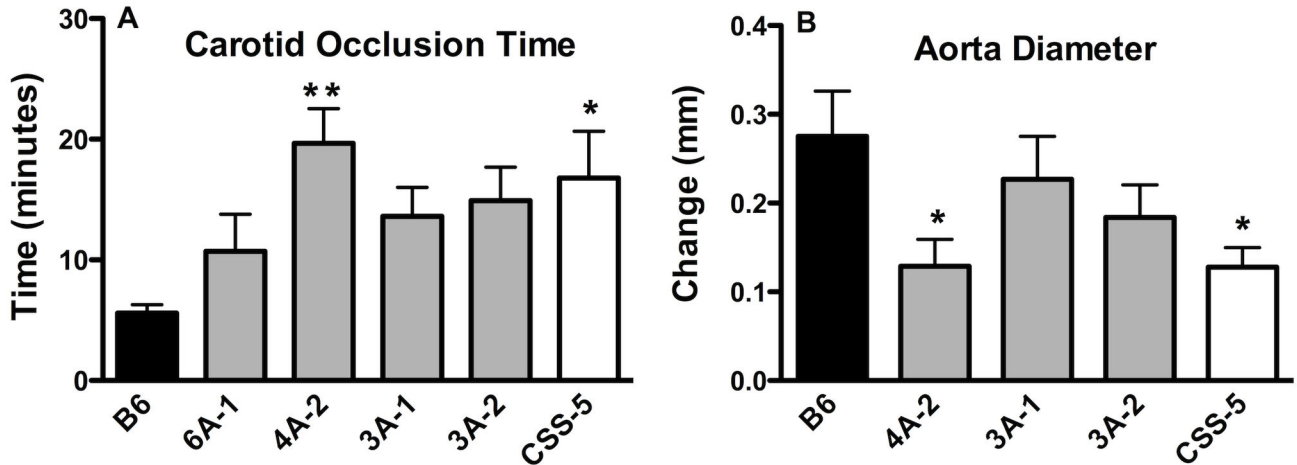
Figure 4. Vascular Injury. A. $FeCl_3$ Induced Carotid Injury Occlusion Time. Time after injury for blood flow to cease. n=5-17. B. $CaCl_2$ Induced Abdominal Aortic Aneurysm. Change in diameter 3wk after $CaCl_2$ treatment. n=7-18, values are the mean ± SEM, one-way ANOVA, * P< 0.05, **P<0.01.
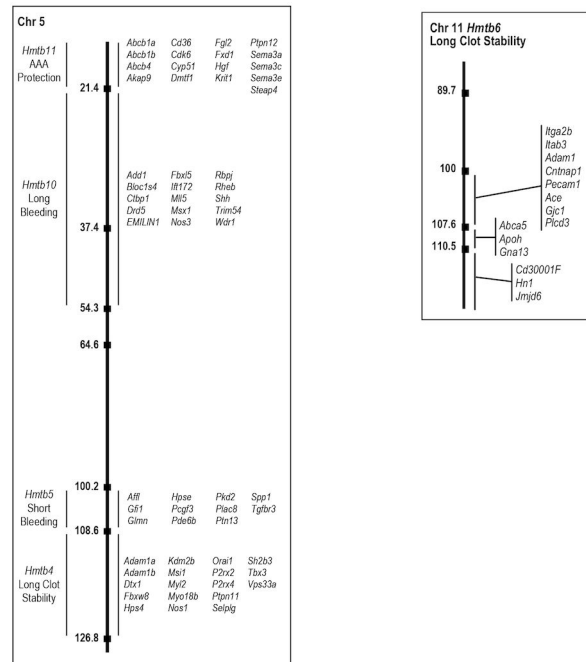doi: 10.1371/journal.pone.0077539.g004
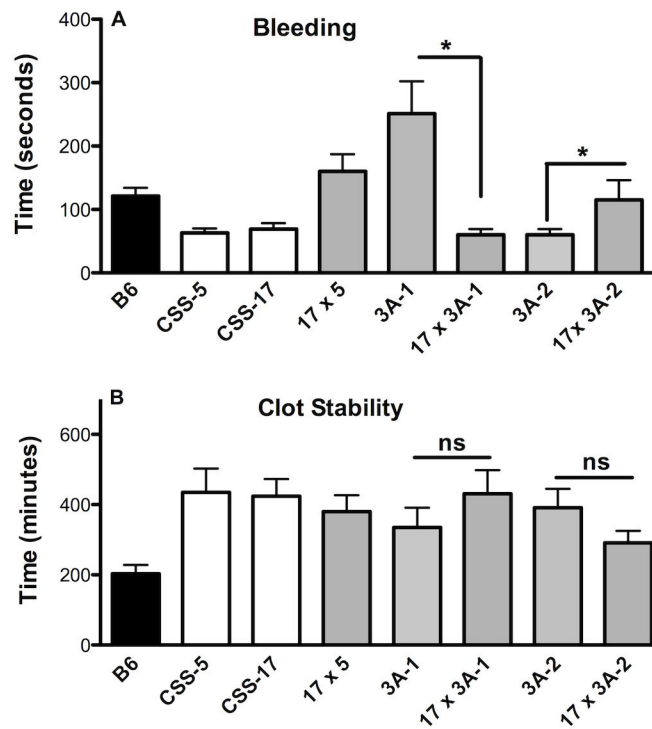
Figure 5. Comparison of Consomic and Congenic crosses. A. First bleeding time. B. Clot Stability-time between first and second bleeding. Values are the mean ± SEM, n=9-24, one-way ANOVA, * P< 0.05.
doi: 10.1371/journal.pone.0077539.g005

The phenotype of the congenic and subcongenic strains demonstrates that the gene (or genes) underlying *Hmtb*6 QTL is located in the distal region on mouse chromosome 11, with a minimum interval of 2.9 Mbp. This region contains 25 known and predicted genes and corresponds closely to a syntenic region on human chromosome 17, from q12 to q25.3. No QTL has been identified in this region in human populations for hemostasis and thrombosis. The only gene known to be related to hemostasis and thrombosis on mouse chromosome 11 is *Serpinf2* (α_2-antiplasmin), an inhibitor of plasmin, the primary

Figure 6. Summary QTL and Candidate Genes for Thrombosis and Hemostasis on Mouse Chromosome 5 and Chromosome 11.

doi: 10.1371/journal.pone.0077539.g006

enzyme for clot lysis. *Serpinf2* is located at 75.2 Mbp and was excluded from the candidates for this trait from our previous study [36]. This conclusion was further confirmed in our current study. Interestingly, Mohlke et al. [43] identified a QTL, *Mvwf* as a modifier of von Willebrand factor (VWF), that regulates plasma VWF level on mouse chromosome 11, in a region between markers *Ngfr* and *Hoxb9* (95.5-96.2 Mbp). They further found that alterations in *Galgt2*, a candidate at the QTL locus at 95.8 Mbp on chromosome 11, influenced plasma VWF levels [44]. This locus was noted in the *Hmtb6* QTL in the previous study [36], and our current study clearly demonstrates that *Mvwf* is located proximal to the *Hmtb6* locus and outside the maximal interval (100-121.8 Mbp), indicating that a gene (or genes) other than *Mvwf* on chromosome 11 regulates hemostasis and thrombosis. Annotation analysis revealed 3 genes in the *Hmtb6* QTL, *Abca5*, *Apoh*, and *Gna13*. *Abca5* deficient mice develop a dilated cardiomyopathy with large thrombi [45,46]. *Gna13* plays a role in platelet -granule release [47-49]. *Apoh*, more commonly known as beta-2-glycoprotein 1, binds to cardiolipin, inhibits platelets activation, and is involved in anticoagulation [50-52]. These genes have not been commonly associated with thrombosis or hemostasis in humans, and may be novel modifiers. In addition to *Abca5* there are 4 other ATP-binding cassette proteins, and besides *Gna13*, *Rgs9* is also associated with G-protein signaling. Three genes are involved in calcium transport, *Cacng1*, *Cacng4* and Cacng5, and three genes code for protein kinases, *Map2k6*, *Prkar1a*, and *Prkca*. *Wipi1* and *Arsg* are associated with the Golgi and endoplasmic reticulum. In the regions of uncertain genotypes of Hmtb6, there were three genes, *Itga2b*, *Itgb3*, and *Pecam-1* that are associated with bleeding and thrombosis. Mutations of *Itga2b* and *Itgb3* are assoicated with Glanzmann thrombasthenia, the most common inherited disease of platelet function in humans, causing a bleeding disorder [53]. *Pecam-1* deficient mice have reduced occlusion time in the formation of a thrombus [54].

Previously [36] we detected a significant locus, Hmtb4, on mouse chromosome 5 for clot stability with a 1-LOD confidence interval 55-66 cM (112.9-127.6 Mbp). From the congenic mapping we confirmed the phenotype of this locus with

increased clot stability similar to the consomic strain CSS-5, compared to the parental strain, B6 mice. Functional annotation analysis identified 18 relevant genes. Genes associated with human syndromes or diseases include: polymorphisms in *Hps4* and *Vps33a* genes, which are, associated with Hermansky-Pudlak syndrome type 4 and the absence of platelet dense granules [9,55]. Orai, the major calcium channel in the platelet plasma membrane, has recently been reported to play a role in platelet activation and thrombus formation [56]. *Ptpn11* is a member of the protein tyrosine phosphatase family, and mutations are identified with Noonan syndrome, one of the most common genetic disorders of congenital heart defects [37,57]. Mice homozygous null for *P2rx4*, a purinergic receptor, ligand gated ion channel 4, have hypertension, abnormal artery morphology and vascular remodeling [58]. The *Sh2b3*, adaptor protein 3 or LNK deficient mice have normal tail bleeding time, but in 60% of the deficient mice rebleeding occurred within 60 seconds, suggesting the clot was unstable. In the 3A-2 congenic strain tail bleeding was reduced and rebleeding inhibited, but similar to the Lnk-/- mice, $FeCl_2$-induced occlusion time was higher in the CSS-5 mice than in B6 mice and similar to the 3A-2 mice. *Selplg* (P-selectin) is a cell adhesion molecule stored in -granules in platelets and Weibel-Palade bodies in endothelial cells and when these cells are activated P-selectin is released to the surface [59,60]. P-selectin is important in the recruitment of leukocytes to sites of injury [61]. *Adam1a* and *Adam1b* have disintegrin metallopeptidase domains that have been implicated as inhibitors of blood coagulation, but these two proteins have not previously been associated with coagulation [62]. From the previous study mapping the QTLs, the region of the 126.8 -138.6 Mbp was outside the 95% confidence region for the *Hmtb4* [36]. The annotated gene in this region was PAI-1, and we did not find any difference in mRNA expression of PAI-1 in the parent strains, and PAI-1 antigen was not different in the congenic strains. It's not likely this is the candidate gene in this QTL. Although considered outside the region of confidence from the previous QTL mapping, there are two known genes that could be candidate genes, *Pf4* and *Pdgfr*, in the proximal region of uncertain genotype in 3A-2.

Hmtb5 locus for bleeding with 1-LOD confidence interval, 45-75 cM (113-128 Mbp) at the distal end of chromosome 5, was previously identified [36]. The congenic strain, 3A-2 with the A/J interval of 100.2-108.6 Mbp, had a short bleeding time similar to the CSS-5 mice suggesting this region was the site of the suppressed bleeding time phenotype in CSS-5. In the subcongenic strain, 2A-1, bleeding time was similar to B6 mice. In the region (100.2-108.6Mbp) of 3A-2 that did not overlap with 2A-1 there were 11 annotated genes for Hmtb5. A potential candidate gene in this region is Hpse, *heparanase*, alpha-endoglucuronidase, a the major enzyme for heparin sulfate degradation. Diabetes and vascular injury increase the expression of *heparanase* and transgenic mice with overexpression of *heparanase* increase thrombosis after mild vascular injury [63,64].

This study has identified a new QTL, *Hmtb5* for bleeding in the proximal region of chromosome 5. From the congenic mapping we confirmed the locus identified at the RFLP marker,

r*s1680965*, in the QTL mapping for long bleeding time. Annotation analysis identified 15 genes in this region. Two of these genes are associated with blood pressure regulation, Drd5 [62,65] and Nos3 [66-68]. The cappuccino deficiency, a spontaneous mutation of Bloc1s4, is associated with reduced platelet dense granules and prolonged bleeding [69,70]. Another gene of interest is EMILIN1. We identified EMILIN2, with a high homology to EMILIN1, in the QTL on chromosome 17 [71,72], in the Hmtb8 locus and found a thrombosis phenotype. The results of the tail bleeding/rebleeding assay and $FeCl_3$ injury model in EMILIN1 deficient mice were not different than for B6 mice (Table S9) suggesting EMILIN1 is not a causative gene in this QTL.

An additional new QTL was uncovered, *Hmtb11* in the congenic strain, 4A-2, that had an increased occlusion time in the carotid injury model and was protected from abdominal aneurysm after $CaCl_2$ injury, which suggests another locus in the proximal region. Genes of particular note from the annotation search are *CD36* that is associated with platelet glycoprotein IV deficiency [73]. *Fgl2*, fibrinogen-like protein2, contributes to immunologically mediated thrombosis in experimental and human viral hepatitis [74].

Limitations of study and future directions

Using congenic and subcongenic mice from two consomic strains, CSS-11 and CSS-5, three QTLs and two additional QTLs were fine-mapped for thrombosis and hemostasis modifiers. Sixty-four potential candidate genes were identified. The limitation of the study is that the causative gene has yet to be identified. Further fine mapping is needed with additional subcongenic strains, as well as expression QTL analysis and quantitative RT-PCR. Future directions will include identification of underlying polymorphisms located in the coding, noncoding or regulatory regions and translating these findings to variation in human genes to assess the relationship of genetic variation to hemostasis and thrombosis risk.

Supporting Information

Table S1.   Genetic Markers and their Chromosomal Position.
(DOCX)

Table S2. RFLP Markers on Chr 5, Primers and Restriction Endonucleases.
(DOCX)

Table S3. Protein–coding Genes, *Hmtb6*, Chromosome 11 100-122Mbp.
(DOCX)

Table S4. Protein-coding Genes, *Hmtb5*, Chromosome 5, 100.2-108.6 Mbp.
(DOCX)

Table S5. Protein-coding Genes, *Hmtb10*, Chromosome 5, 21.4-54.3 Mbp.

(DOCX)

Table S6. Protein-coding Genes, *Hmtb4*, Chromosome 5, 108-126.8 Mbp.
(DOCX)

Table S7. Protein-coding Genes Non-overlapping Region 4A-2, *Hmtb11*, Chromosome 5, 54.3-64.6 Mbp.
(DOCX)

Table S8. Protein-coding Genes, *Hmtb11*, Protein-coding Genes, Chromosome 5, 0-21.4.

Table S9. Candidate gene, Emilin1.
(DOCX)

Author Contributions

Conceived and designed the experiments: JHP QS MH. Performed the experiments: JHP QS MH JG. Analyzed the data: JHP QS MH JG. Wrote the manuscript: JHP QS MH.

References

1. Marenberg ME, Risch N, Berkman LF, Floderus B, de Faire U (1994) Genetic susceptibility to death from coronary heart disease in a study of twins. N Engl J Med 330: 1041-1046. doi:10.1056/NEJM199404143301503. PubMed: 8127331.
2. Voetsch B, Loscalzo J (2004) Genetic determinants of arterial thrombosis. Arterioscler Thromb Vasc Biol 24: 216-229. PubMed: 14615395.
3. Rosenberg RD, Aird WC (1999) Vascular-bed--specific hemostasis and hypercoagulable states. N Engl J Med 340: 1555-1564. doi:10.1056/NEJM199905203402007. PubMed: 10332019.
4. Caprini JA, Glase CJ, Anderson CB, Hathaway K (2004) Laboratory markers in the diagnosis of venous thromboembolism. Circulation 109: I4-I8. doi:10.1161/01.CIR.0000122869.59485.36. PubMed: 15051662.
5. Humphries SE, Green FR, Temple A, Dawson S, Henney A et al. (1992) Genetic factors determining thrombosis and fibrinolysis. Ann Epidemiol 2: 371-385. doi:10.1016/1047-2797(92)90086-6. PubMed: 1342288.
6. Nesheim M (2003) Thrombin and fibrinolysis. Chest 124: 33S-39S. doi:10.1378/chest.124.3_suppl.33S. PubMed: 12970122.
7. Schlager G, Dickie MM (1967) Spontaneous mutations and mutation rates in the house mouse. Genetics 57: 319-330. PubMed: 4869340.
8. Hoover-Plow J (1980) Phosphorylase kinase deficiency and decreased fat accumulation in hybrid male mice (I X C3H). Proc Soc Exp Biol Med 165: 409-412. doi:10.3181/00379727-165-40996. PubMed: 7465553.
9. Novak EK, Hui SW, Swank RT (1984) Platelet storage pool deficiency in mouse pigment mutations associated with seven distinct genetic loci. Blood, 63: 536-544. PubMed: 6696991.
10. Hoover-Plow J, Skomorovska-Prokvolit O, Welsh S (2001) Selective behaviors altered in plasminogen-deficient mice are reconstituted with intracerebroventricular injection of plasminogen. Brain Res 898: 256-264. doi:10.1016/S0006-8993(01)02191-6. PubMed: 11306011.
11. Weinbaum JS, Broekelmann TJ, Pierce RA, Werneck CC, Segade F et al. (2008) Deficiency in microfibril-associated glycoprotein-1 leads to complex phenotypes in multiple organ systems. J Biol Chem 283: 25533-25543. doi:10.1074/jbc.M709962200. PubMed: 18625713.
12. Hughes SD, Verstuyft J, Rubin EM (1997) HDL deficiency in genetically engineered mice requires elevated LDL to accelerate atherogenesis. Arterioscler Thromb Vasc Biol 17: 1725-1729. doi:10.1161/01.ATV.17.9.1725. PubMed: 9327769.
13. Hoover-Plow JL, Gong Y, Shchurin A, Busuttil SJ, Schneeman TA et al. (2008) Strain and model dependent differences in inflammatory cell recruitment in mice. Inflamm Res 57: 457-463. doi:10.1007/s00011-008-7062-5. PubMed: 18827970.
14. Ginsburg D (2005) Identifying novel genetic determinants of hemostatic balance. J Thromb Haemost 3: 1561-1568. doi:10.1111/j.1538-7836.2005.01461.x. PubMed: 16102020.
15. Lander ES, Green P, Abrahamson J, Barlow A, Daly MJ et al. (1987) MAPMAKER: an interactive computer package for constructing primary genetic linkage maps of experimental and natural populations. Genomics 1: 174-181. doi:10.1016/0888-7543(87)90010-3. PubMed: 3692487.
16. Moore KJ, Nagle DL (2000) Complex trait analysis in the mouse: The strengths, the limitations and the promise yet to come. Annu Rev Genet 34: 653-686. doi:10.1146/annurev.genet.34.1.653. PubMed: 11092842.
17. Mehrabian M, Wen PZ, Fisler J, Davis RC, Lusis AJ (1998) Genetic loci controlling body fat, lipoprotein metabolism, and insulin levels in a multifactorial mouse model. J Clin Invest 101: 2485-2496. doi:10.1172/JCI1748. PubMed: 9616220.
18. Almind K, Kulkarni RN, Lannon SM, Kahn CR (2003) Identification of interactive loci linked to insulin and leptin in mice with genetic insulin resistance. Diabetes 52: 1535-1543. doi:10.2337/diabetes.52.6.1535. PubMed: 12765967.
19. Warden CH, Fisler JS, Shoemaker SM, Wen PZ, Svenson KL et al. (1995) Identification of four chromosomal loci determining obesity in a multifactorial mouse model. J Clin Invest 95: 1545-1552. doi:10.1172/JCI117827. PubMed: 7706460.
20. Mu JL, Naggert JK, Svenson KL, Collin GB, Kim JH et al. (1999) Quantitative trait loci analysis for the differences in susceptibility to atherosclerosis and diabetes between inbred mouse strains C57BL/6J and C57BLKS/J. J Lipid Res 40: 1328-1335. PubMed: 10393218.
21. Lembertas AV, Pérusse L, Chagnon YC, Fisler JS, Warden CH et al. (1997) Identification of an obesity quantitative trait locus on mouse chromosome 2 and evidence of linkage to body fat and insulin on the human homologous region 20q. J Clin Invest 100: 1240-1247. doi:10.1172/JCI119637. PubMed: 9276742.
22. Mehrabian M, Wong J, Wang X, Jiang Z, Shi W et al. (2001) Genetic locus in mice that blocks development of atherosclerosis despite extreme hyperlipidemia. Circ Res 89: 125-130. doi:10.1161/hh1401.093458. PubMed: 11463718.
23. Purcell-Huynh DA, Weinreb A, Castellani LW, Mehrabian M, Doolittle MH et al. (1995) Genetic factors in lipoprotein metabolism. Analysis of a genetic cross between inbred mouse strains NZB/BINJ and SM/J using a complete linkage map approach. J Clin Invest 96: 1845-1858. doi:10.1172/JCI118230. PubMed: 7560076.
24. Naggert JK, Mu JL, Frankel W, Bailey DW, Paigen B (1995) Genomic analysis of the C57BL/Ks mouse strain. Mamm Genome 6: 131-133. doi:10.1007/BF00303258. PubMed: 7766997.
25. Allayee H, Ghazalpour A, Lusis AJ (2003) Using mice to dissect genetic factors in atherosclerosis. Arterioscler Thromb Vasc Biol 23: 1501-1509. doi:10.1161/01.ATV.0000090886.40027.DC. PubMed: 12920046.
26. Smith J (2003) Quantitative trait locus mapping for atherosclerosis susceptibility. Curr Opin Lipidol 14: 499-504. doi:10.1097/00041433-200310000-00011. PubMed: 14501589.
27. Smith JD, James D, Dansky HM, Wittkowski KM, Moore KJ et al. (2003) In silico quantitative trait locus map for atherosclerosis susceptibility in apolipoprotein E-deficient mice. Arterioscler Thromb Vasc Biol 23: 117-122. doi:10.1161/01.ATV.0000047461.18902.80. PubMed: 12524234.
28. Smith JD, Bhasin JM, Baglione J, Settle M, Xu Y et al. (2006) Atherosclerosis susceptibility loci identified from a strain intercross of apolipoprotein E-deficient mice via a high-density genome scan. Arterioscler Thromb Vasc Biol 26: 597-603. PubMed: 16373612.
29. Chiu S, Kim K, Haus KA, Espinal GM, Millon LV et al. (2007) Identification of positional candidate genes for body weight and adiposity in subcongenic mice. Arterioscler Thromb Vasc Biol 31: 75-85. PubMed: 17536020.
30. Cheli Y, Kunicki TJ (2006) hnRNP L regulates differences in expression of mouse integrin alpha2beta1. Blood 107: 4391-4398. doi:10.1182/blood-2005-12-4822. PubMed: 16455949.
31. Nadeau JH, Singer JB, Matin A, Lander ES (2000) Analysing complex genetic traits with chromosome substitution strains. Nat Genet 24: 221-225. doi:10.1038/73427. PubMed: 10700173.
32. Mouzeyan A, Choi J, Allayee H, Wang X, Sinsheimer J et al. (2000) A locus conferring resistance to diet-induced hypercholesterolemia and

atherosclerosis on mouse chromosome 2. J Lipid Res 41: 573-582. PubMed: 10744778.

33. Nadeau JH, Arbuckle LD, Skamene E (1995) Genetic dissection of inflammatory responses. J Inflamm 45: 27-48. PubMed: 7583351.

34. Singer JB, Hill AE, Burrage LC, Olszens KR, Song J et al. (2004) Genetic dissection of complex traits with chromosome substitution strains of mice. Science 304: 445-448. doi:10.1126/science.1093139. PubMed: 15031436.

35. Hoover-Plow J, Shchurin A, Hart E, Sha J, Hill AE et al. (2006) Genetic background determines response to hemostasis and thrombosis. BMC Blood Disord, 6: 6. doi:10.1186/1471-2326-6-6. PubMed: 17022820.

36. Sa Q, Hart E, Hill AE, Nadeau JH, Hoover-Plow JL (2008) Quantitative trait locus analysis for hemostasis and thrombosis. Mamm Genome 19: 406-412. doi:10.1007/s00335-008-9122-0. PubMed: 18787898.

37. Eppig JT, Blake JA, Bult CJ, Kadin JA, Richardson JE (2012) The Mouse Genome Database (MGD): comprehensive resource for genetics and genomics of the laboratory mouse. Nucleic Acids Res 40: D881-D886. doi:10.1093/nar/gkr974. PubMed: 22075990.

38. Huang da W, Sherman BT, Lempicki RA (2009) Systematic and integrative analysis of large gene lists using DAVID bioinformatics resources. Nat Protoc 4: 44-57. PubMed: 19131956.

39. Gong Y, Hart E, Shchurin A, Hoover-Plow J (2008) Inflammatory macrophage migration requires MMP-9 activation by plasminogen in mice. J Clin Invest 118: 3012-3024. doi:10.1172/JCI32750. PubMed: 18677407.

40. Buchner DA, Burrage LC, Hill AE, Yazbek SN, O'Brien WE et al. (2008) Resistance to diet-induced obesity in mice with a single substituted chromosome. Physiol Genomics 35: 116-122. doi:10.1152/physiolgenomics.00033.2008. PubMed: 18628339.

41. Buchner DA, Yazbek SN, Solinas P, Burrage LC, Morgan MG et al. (2011) Increased mitochondrial oxidative phosphorylation in the liver is associated with obesity and insulin resistance. Obesity (Silver Spring) 19: 917-924. doi:10.1038/oby.2010.214. PubMed: 20885388.

42. Yazbek SN, Buchner DA, Geisinger JM, Burrage LC, Spiezio SH et al. (2011) Deep congenic analysis identifies many strong, context-dependent QTLs, one of which, Slc35b4, regulates obesity and glucose homeostasis. Genome Res 21: 1065-1073. doi:10.1101/gr.120741.111. PubMed: 21507882.

43. Mohlke KL, Nichols WC, Westrick RJ, Novak EK, Cooney KA et al. (1996) A novel modifier gene for plasma von Willebrand factor level maps to distal mouse chromosome 11. Proc Natl Acad Sci U S A 93: 15352-15357. doi:10.1073/pnas.93.26.15352. PubMed: 8986815.

44. Mohlke KL, Purkayastha AA, Westrick RJ, Smith PL, Petryniak B et al. (1999) Mvwf, a dominant modifier of murine von Willebrand factor, results from altered lineage-specific expression of a glycosyltransferase. Cell 96: 111-120. doi:10.1016/S0092-8674(00)80964-2. PubMed: 9989502.

45. Eren M, Painter CA, Atkinson JB, Declerck PJ, Vaughan DE (2002) Age-dependent spontaneous coronary arterial thrombosis in transgenic mice that express a stable form of human plasminogen activator inhibitor-1. Circulation 106: 491-496. doi:10.1161/01.CIR.0000023186.60090.FB. PubMed: 12135951.

46. Kubo Y, Sekiya S, Ohigashi M, Takenaka C, Tamura K et al. (2005) ABCA5 resides in lysosomes, and ABCA5 knockout mice develop lysosomal disease-like symptoms. Mol Cell Biol 25: 4138-4149. doi:10.1128/MCB.25.10.4138-4149.2005. PubMed: 15870284.

47. Dorsam RT, Kim S, Jin J, Kunapuli SP (2002) Coordinated signaling through both G12/13 and G(i) pathways is sufficient to activate GPIIb/IIIa in human platelets. J Biol Chem 277: 47588-47595. doi:10.1074/jbc.M208778200. PubMed: 12297512.

48. Quinton TM, Murugappan S, Kim S, Jin J, Kunapuli SP (2004) Different G protein-coupled signaling pathways are involved in alpha granule release from human platelets. J Thromb Haemost 2: 978-984. doi:10.1111/j.1538-7836.2004.00741.x. PubMed: 15140134.

49. Ruppel KM, Willison D, Kataoka H, Wang A, Zheng YW et al. (2005) Essential role for Galpha13 in endothelial cells during embryonic development. Proc Natl Acad Sci U S A 102: 8281-8286. doi:10.1073/pnas.0503326102. PubMed: 15919816.

50. Borchman D, Harris EN, Pierangeli SS, Lamba OP (1995) Interactions and molecular structure of cardiolipin and beta 2-glycoprotein 1 (beta 2-GP1). Clin Exp Immunol 102: 373-378. PubMed: 7586693.

51. Mori T, Takeya H, Nishioka J, Gabazza EC, Suzuki K (1996) beta 2-Glycoprotein I modulates the anticoagulant activity of activated protein C on the phospholipid surface. Thromb Haemost 75: 49-55. PubMed: 8713779.

52. Nimpf J, Wurm H, Kostner GM (1985) Interaction of beta 2-glycoprotein-I with human blood platelets: influence upon the ADP-induced aggregation. Thromb Haemost 54: 397-401. PubMed: 4082080.

53. Nurden AT, Pillois X, Nurden P (2012) Understanding the genetic basis of Glanzmann thrombasthenia: implications for treatment. Expert. Rev Hematol 5: 487-503.

54. Falati S, Patil S, Gross PL, Stapleton M, Merrill-Skoloff G et al. (2006) Platelet PECAM-1 inhibits thrombus formation in vivo. Blood 107: 535-541. doi:10.1182/blood-2005-04-1512. PubMed: 16166583.

55. Anderson PD, Huizing M, Claassen DA, White J, Gahl WA (2003) Hermansky-Pudlak syndrome type 4 (HPS-4): clinical and molecular characteristics. Hum Genet 113: 10-17. PubMed: 12664304.

56. Braun A, Vogtle T, Varga-Szabo D, Nieswandt B (2011) STIM and Orai in hemostasis and thrombosis. Front Biosci 16: 2144-2160. doi:10.2741/3844. PubMed: 21622167.

57. Araki T, Mohi MG, Ismat FA, Bronson RT, Williams IR et al. (2004) Mouse model of Noonan syndrome reveals cell type- and gene dosage-dependent effects of Ptpn11 mutation. Nat Med 10: 849-857. doi:10.1038/nm1084. PubMed: 15273746.

58. Kaczmarek-Hájek K, Lörinczi E, Hausmann R, Nicke A (2012) Molecular and functional properties of P2X receptors--recent progress and persisting challenges. Purinergic Signal 8: 375-417. doi:10.1007/s11302-012-9314-7. PubMed: 22547202.

59. Cleator JH, Zhu WQ, Vaughan DE, Hamm HE (2006) Differential regulation of endothelial exocytosis of P-selectin and von Willebrand factor by protease-activated receptors and cAMP. Blood 107: 2736-2744. doi:10.1182/blood-2004-07-2698. PubMed: 16332977.

60. Rhea KE (1991) Noninvasive vascular studies. J Ultrasound Med 10: 316. PubMed: 1895372.

61. Furie B, Furie BC (1996) P-selectin induction of tissue factor biosynthesis and expression. Haemostasis 26 Suppl 1: 60-65. PubMed: 8904175.

62. Kim E, Nishimura H, Baba T (2003) Differential localization of ADAM1a and ADAM1b in the endoplasmic reticulum of testicular germ cells and on the surface of epididymal sperm. Biochem Biophysl Res Commun 304: 313-319. doi:10.1016/S0006-291X(03)00588-6. PubMed: 12711316.

63. Baker AB, Gibson WJ, Kolachalama VB, Golomb M, Indolfi L et al. (2012) Heparanase regulates thrombosis in vascular injury and stent-induced flow disturbance. J Am Coll Cardiol 59: 1551-1560. doi:10.1016/j.jacc.2011.11.057. PubMed: 22516446.

64. Baker AB, Groothuis A, Jonas M, Ettenson DS, Shazly T et al. (2009) Heparanase alters arterial structure, mechanics, and repair following endovascular stenting in mice. Circ Res, 104: 380-387. doi:10.1161/CIRCRESAHA.108.180695. PubMed: 19096032.

65. Hollon TR, Bek MJ, Lachowicz JE, Ariano MA, Mezey E et al. (2002) Mice lacking D5 dopamine receptors have increased sympathetic tone and are hypertensive. J Neurosci 22: 10801-10810. PubMed: 12486173.

66. Shesely EG, Maeda N, Kim HS, Desai KM, Krege JH et al. (1996) Elevated blood pressures in mice lacking endothelial nitric oxide synthase. Proc Natl Acad Sci U S A 93: 13176-13181. doi:10.1073/pnas.93.23.13176. PubMed: 8917564.

67. Gödecke A, Decking UK, Ding Z, Hirchenhain J, Bidmon HJ et al. (1998) Coronary hemodynamics in endothelial NO synthase knockout mice. Circ Res 82: 186-194. doi:10.1161/01.RES.82.2.186. PubMed: 9468189.

68. Huang PL, Huang Z, Mashimo H, Bloch KD, Moskowitz MA et al. (1995) Hypertension in mice lacking the gene for endothelial nitric oxide synthase. Nature 377: 239-242. doi:10.1038/377239a0. PubMed: 7545787.

69. Gwynn B, Ciciotte SL, Hunter SJ, Washburn LL, Smith RS et al. (2000) Defects in the cappuccino (cno) gene on mouse chromosome 5 and human 4p cause Hermansky-Pudlak syndrome by an AP-3-independent mechanism. Blood 96: 4227-4235. PubMed: 11110696.

70. Ciciotte SL, Gwynn B, Moriyama K, Huizing M, Gahl WA et al. (2003) Cappuccino, a mouse model of Hermansky-Pudlak syndrome, encodes a novel protein that is part of the pallidin-muted complex (BLOC-1). Blood 101: 4402-4407. doi:10.1182/blood-2003-01-0020. PubMed: 12576321.

71. Sa Q, Hoover-Plow JL (2011) EMILIN2 (Elastin microfibril interface located protein), potential modifier of thrombosis. Thromb J 9: 9. doi:10.1186/1477-9560-9-9. PubMed: 21569335.

72. Sa Q, Hart E, Nadeau JH, Hoover-Plow JL (2010) Mouse chromosome 17 candidate modifier genes for thrombosis. Mamm Genome 21: 337-349. doi:10.1007/s00335-010-9274-6. PubMed: 20700597.

73. Ghosh A, Murugesan G, Chen K, Zhang L, Wang Q et al. (2011) Platelet CD36 surface expression levels affect functional responses to oxidized LDL and are associated with inheritance of specific genetic polymorphisms. Blood 117: 6355-6366. doi:10.1182/blood-2011-02-338582. PubMed: 21478428.

74. Marsden PA, Ning Q, Fung LS, Luo X, Chen Y et al. (2003) The Fgl2/ fibroleukin prothrombinase contributes to immunologically mediated thrombosis in experimental and human viral hepatitis. J Clin Invest 112: 58-66. doi:10.1172/JCI200318114. PubMed: 12840059.